

Accepted Manuscript

Morphological and biomolecular evidence for tuberculosis in 8th century AD skeletons from Bélmegyer-Csömöki domb, Hungary

Erika Molnár, Helen D. Donoghue, Oona Y-C. Lee, Houdini H.T. Wu, Gurdyal S. Besra, David E. Minnikin, Ian D. Bull, Gareth Llewellyn, Christopher M. Williams, Olga Spekker, György Pálfi

PII: S1472-9792(15)00033-5

DOI: [10.1016/j.tube.2015.02.032](https://doi.org/10.1016/j.tube.2015.02.032)

Reference: YTUBE 1293

To appear in: *Tuberculosis*



Please cite this article as: Molnár E, Donoghue HD, Lee OY-C, Wu HHT, Besra GS, Minnikin DE, Bull ID, Llewellyn G, Williams CM, Spekker O, Pálfi G, Morphological and biomolecular evidence for tuberculosis in 8th century AD skeletons from Bélmegyer-Csömöki domb, Hungary, *Tuberculosis* (2015), doi: 10.1016/j.tube.2015.02.032.

This is a PDF file of an unedited manuscript that has been accepted for publication. As a service to our customers we are providing this early version of the manuscript. The manuscript will undergo copyediting, typesetting, and review of the resulting proof before it is published in its final form. Please note that during the production process errors may be discovered which could affect the content, and all legal disclaimers that apply to the journal pertain.

1 **Morphological and biomolecular evidence for tuberculosis in 8th century AD skeletons from**
2 **Bélmegyer-Csömöki domb, Hungary**

3

4 Erika Molnár^{a*}, Helen D. Donoghue^b, Oona Y-C. Lee^c, Houdini H.T. Wu^c, Gurdyal S. Besra^c,
5 David E. Minnikin^c, Ian D. Bull^d, Gareth Llewellyn^e, Christopher M. Williams^e, Olga Spekker^a and
6 György Pálfi^a

7

8

9 ^aDepartment of Biological Anthropology, University of Szeged, Szeged, Hungary

10 ^bCentre for Clinical Microbiology and Centre for the History of Medicine, University College
11 London, London, UK

12 ^cInstitute of Microbiology and Infection, School of Biosciences, University of Birmingham,
13 Edgbaston, Birmingham, UK

14 ^dOrganic Geochemistry Unit, School of Chemistry, University of Bristol, Bristol, UK

15 ^eNational Mass Spectrometry Service Centre, School of Medicine, Grove Building, Swansea
16 University, Swansea, UK

17

18

19 Email addresses:

20 balinte@bio.u-szeged.hu; h.donoghue@ucl.ac.uk; o.y.lee@bham.ac.uk; h.wu.2@bham.ac.uk;

21 g.besra@bham.ac.uk; d.e.minnikin@bham.ac.uk; ian.d.bull@bristol.ac.uk;

22 g.llewellyn@swansea.ac.uk; christopher.matthew.williams@swansea.ac.uk;

23 olga.spekker@gmail.com; palfigy@bio.u-szeged.hu

24 *Corresponding author:

25 H-6724, Szeged

26 Közép fasor 52.

27 E-mail : balinte@bio.u-szeged.hu

28 Fax/Telephone : +36 62 544 314

29 Word count summary : 184

30 Word count (excluding summary and references) : 3075

31

ACCEPTED MANUSCRIPT

32 **Summary**

33 Macromorphological analysis of skeletons, from 20 selected graves of the 8th century AD
34 BÉlmegyer-Csömöki domb, revealed 19 cases of possible skeletal tuberculosis. Biomolecular
35 analyses provided general support for such diagnoses, including the individual without pathology,
36 but the data did not show coherent consistency over the range of biomarkers examined.
37 Amplification of ancient DNA fragments found evidence for the *Mycobacterium tuberculosis*
38 complex DNA only in five graves. In contrast, varying degrees of lipid biomarker presence were
39 recorded in all except two of the skeletons, though most lipid components appeared to be somewhat
40 degraded. Mycobacterial mycolic acid biomarkers were absent in five cases, but the weak, possibly
41 degraded profiles for the remainder were smaller and inconclusive for either tuberculosis or leprosy.
42 The most positive lipid biomarker evidence for tuberculosis was provided by mycolipenic acid, with
43 13 clear cases, supported by five distinct possible cases. Combinations of mycocerosic acids were
44 present in all but three graves, but in one case a tuberculosis-leprosy co-infection was indicated. In
45 two specimens with pathology, no lipid biomarker evidence was recorded, but one of these
46 specimens provided *M. tuberculosis* complex DNA fragments.

47

48 **Key words:** ancient DNA; lipid biomarkers; *Mycobacterium tuberculosis* complex;
49 palaeopathology; PCR

50

51 1. Introduction

52 The macromorphological diagnosis of skeletal tuberculosis (TB) in human remains is based upon
53 the detection of secondary skeletal lesions.¹ The most common representation of skeletal TB is
54 spondylitis tuberculosa, which affects the vertebral column. After vertebral involvement, the second
55 most frequent alteration in TB is arthritis of the large, weight-bearing joints.² Initially, the diagnosis
56 of TB in osteoarchaeological samples focused only on these classical TB lesions, representing a
57 fairly developed stage of tuberculosis. However, TB may have affected many individuals without
58 classical pathological changes, thus patients died in an earlier stage of tuberculosis long before
59 these symptoms could have developed. Clearly, this early-stage TB is not recognizable on the basis
60 of classical TB alterations, so if we consider only individuals with visible TB-related lesions, it is
61 likely this will significantly underestimate the prevalence of tuberculosis in the examined historical
62 populations.^{1,3}

63 Because of the problems of tuberculosis diagnostics, the importance of establishing diagnostic
64 criteria for early-stage TB became recognized in the late 20th century. A number of studies – mainly
65 based on the examination of skeletal collections with known causes of death – have focused on
66 searching for atypical or early-stage lesions in connection with tuberculosis infection. These
67 investigations enabled the recognition of three types of atypical or early-stage TB alterations: rib
68 lesions, superficial vertebral changes including hypervascularisation, and endocranial alterations.³⁻⁷
69 Positive correlations between tuberculosis and stress indicators, such as long bone periostitis, *cribra*
70 *orbitalia* and *cribra cranii*, were also recognized.^{7,8} Since the 1990s, the identification of skeletal
71 tuberculosis in ancient human remains has been facilitated by the confirmation of atypical or early-
72 stage TB lesions by new biomolecular methods based on mycobacterial ancient DNA (aDNA) and
73 lipid biomarker analyses.^{1,9-12}

74 In 1990, the first paleopathological analyses of the 8th century AD series Bélmegyer-Csömöki
75 domb were essentially based on macromorphological and radiological examinations, biomolecular
76 methods were used only in a few cases. From a macromorphological point of view, those
77 investigations only considered classical TB alterations.^{9,13,14,15} An advanced-age female skeleton
78 from the grave No. 65 showed severe osteolytic lesions of the anterior portion of the thoracic and
79 lumbar vertebral bodies, causing an unequal collapse, which led to angular kyphosis (Suppl. Fig. S1
80 a-b).¹⁴ Mycobacterial DNA targets IS6110 and the 65-kDa antigen gene, of the *Mycobacterium*
81 *tuberculosis* complex (MTBC), were found in samples from this specimen.⁹ In another case, of a
82 mature male individual (grave No. 90), the pathological remodelling and fusion of the lumbosacral
83 region and the irregular *ante-mortem* erosion on the ventral surface of the sacrum, support the
84 diagnosis of a lumbo-sacral tuberculous involvement with cold abscess. In addition, the severe
85 destruction both of the left hip bone and proximal femur is suggestive of tuberculous arthritis or
86 *coxitis tuberculosa* (Suppl. Fig. S1 c-d).¹⁵ The diagnosis of skeletal TB was confirmed by
87 biomolecular results, the identification of the DNA-fragment (65-kDa antigen gene) of the MTBC
88 was successful.⁹ In a further case, the complete ankylosis of the right knee indicated *gonitis*
89 *tuberculosa* of an elderly male individual from grave No. 215.¹³

90 Marcsik and co-workers published two further classical TB cases in 2007.¹⁶ A young female
91 skeleton from grave No. 38 exhibited signs of probable tuberculous arthritis (*coxitis tuberculosa*) of
92 the right hip joint. Skeletal remains of an adult male individual (grave No. 189) presented complete
93 ankylosis of the 9th and 10th thoracic vertebrae and fusion of the 1st and 2nd and the 3rd and 4th
94 lumbar vertebrae. In addition, new bone formation and osteophytes were found on the ventral
95 surfaces of all lumbar vertebral bodies. These alterations suggest the diagnosis of spondylitis
96 *tuberculosa*.¹⁶

97 The above mentioned former investigations of the series from the Bélmegyer-Csömöki domb
98 have provided interesting paleopathological cases of skeletal tuberculosis. However, the complete

99 skeletal material has never been analysed systematically for both classical and early-stage TB
100 lesions, and biomolecular analyses had been undertaken only in a few cases. The recent
101 development of diagnostic criteria in the field of paleopathology of TB and biomolecular methods
102 for detection of the MTBC encouraged us to perform a re-examination of the series from 2009. The
103 aim of this study is to summarize the results of this re-examination.

104 **2. Material and Methods**

105 *2.1 Archaeological background*

106 The skeletal material for this study derives from the archaeological site of the BÉlmeqyer-
107 Csömöki domb, rising about three kilometres south-east of the village BÉlmeqyer, in South-Eastern
108 Hungary. During a long-running excavation (1985 – 1989), skeletal remains of 240 individuals
109 were unearthed. On the basis of the grave goods found in the completely excavated cemetery, it was
110 used for burials between 670 – 800 AD during the late Avar Period.^{17,18}

111 Our research strategy was to combine different diagnostic methods in order to get independent
112 verification using different biomarkers. First we conducted the morphological analysis of the
113 skeletal series. Next, bone samples were taken from the skeletal remains of the suspected TB cases.
114 Small pieces from the same rib were selected and sent to separate centres for the aDNA and lipid
115 biomarker analyses.

116 *2.2 Macromorphological analysis*

117 The paleopathological examination of the mostly well-preserved skeletal remains of the 240
118 individuals (95 males, 72 females, 73 undeterminable) was carried out in the Department of
119 Biological Anthropology, University of Szeged, Hungary. These investigations were performed
120 using macromorphological methods, focussing on previously detailed classical² and atypical TB
121 alterations.³⁻⁷

122 2.3 *Mycobacterial aDNA analysis*

123 2.3.1 *Mycobacterial DNA extraction*

124 Possible cases of skeletal TB, defined according to skeletal morphological alterations, were
125 examined for the presence of aDNA from the *Mycobacterium tuberculosis* complex (MTBC).
126 Recommended protocols for aDNA work were followed¹⁹ with separate rooms and equipment for
127 different stages of the process. Well-established methods were employed for aDNA extraction and
128 amplification²⁰⁻²⁷ as detailed in Donoghue *et al* in this volume²⁸ and in Supplementary data. The
129 approach used was of a slow but thorough period of sample disruption, one aliquot treated with N-
130 phenacylthiozolium bromide (PTB), to cleave any covalent cross-links thus facilitating DNA strand
131 separation and amplification.²¹ Subsequently, samples were treated with guanidium thiocyanate,
132 followed by sample and bacterial cell disruption, using boiling and snap-freezing in liquid nitrogen.
133 All fractions of the sample were used in the extraction. DNA was captured with silica and the
134 pellets washed and dried.²⁸ Silica supernates from PTB-negative samples were also processed by
135 removal of protein followed by DNA precipitation with isopropanol (−20 °C).²⁸ Dried samples were
136 re-hydrated with elution buffer and used immediately or stored at −20 °C. Negative extraction
137 controls were processed in parallel with the test samples.

138 2.3.2 *DNA amplification and detection*

139 Two specific regions of the *M. tuberculosis* complex were targeted – the repetitive elements
140 IS6110 (1–25 copies/cell) and IS1081 (6 copies/cell). The IS6110 primers used for conventional
141 PCR had a target region of 123 bp²² and the IS1081 primers produce an amplicon of 113 bp.²³
142 Later, specific *M. tuberculosis* primers and a fluorescent probe were used²⁴ to enable shorter DNA
143 fragments to be detected in a real-time PCR reaction (Supplementary data).

144 2.3.3 *The PCR conditions*

145 The PCR mix included 2mM bovine serum albumin to reduce PCR inhibition²⁵ and 2.0mM
146 MgCl₂. PCR assays were initially run at an annealing temperature of 58°C and amplified DNA was

147 examined by agarose gel electrophoresis.²⁶ Subsequently, amplification was performed in a final
148 volume of 25µl using a RotorGene[®] 3000 (Qiagen) real-time platform²⁷ to enable the detection of
149 DNA using SYBR Green and melt analysis or specific primers with fluorescent probe. Annealing
150 was at 60°C. A hot-start *Taq* polymerase was used to minimize non-specific primer and template
151 binding. Negative DNA extraction and PCR controls were processed alongside the test samples.

152 2.4 Lipid Biomarker Analysis

153 Details of the methods and analysis are given in the Supplementary data. Specimens were
154 hydrolysed by heating with 30% potassium hydroxide in methanol (2ml) and toluene (1ml) at 100°C
155 overnight.^{11,29} In parallel, standard biomass of *M. tuberculosis* and *M. leprae* was processed. Long-
156 chain compounds were extracted as described previously²⁹ and the extract was treated with
157 pentafluorobenzyl bromide, under phase-transfer conditions^{11,29} to convert acidic components into
158 pentafluorobenzyl (PFB) esters. Subsequent separation on an Alltech 209250 (500mg) normal phase
159 silica gel cartridge gave fractions containing non-hydroxylated fatty acid PFB esters, mycolic acid
160 (MA) PFB esters and free phthiocerols.^{11,29} The MA PFB esters reacted with pyrenebutyric acid
161 fi(PBA) to produce PBA-PFB MA derivatives, which were purified on an Alltech 205250 (500mg)
162 C₁₈ reverse phase cartridge.^{11,29} The PBA-PFB mycolates were analysed by reverse phase HPLC,
163 as described previously.^{11,29} The non-hydroxylated PFB ester fractions were refined on an Alltech
164 205250 (500mg) reverse phase silica gel cartridge, using a water-methanol/methanol/methanol-
165 toluene elution sequence.²⁹ A fraction enriched in mycocerosic acid and other longer chain (> C₂₀)
166 PFB esters was eluted by 100% methanol with the more usual C₁₂ to C₂₀ esters eluting in the earlier
167 water/methanol fractions. The fractions containing possible mycocerosates, were analysed by
168 negative ion chemical ionization gas chromatography mass spectrometry (NICI-GCMS), as
169 previously described.²⁹

170 3. Results

171 3.1 Macromorphological analysis

172 During the macromorphological analysis of the skeletal material of the BÉlmegyer-Csömöki
173 domb, 19 cases of probable skeletal tuberculosis were detected. Classical TB changes were
174 observed in the five cases detailed above in the Introduction (Suppl. Fig. S1 a-d; Table 1), while
175 atypical or early-stage TB lesions were observed in a further 14 cases (Suppl. Fig. S2 a-c; Table 1).
176 It is clear, therefore, that these atypical or early TB changes occurred significantly more often than
177 the classical alterations. Only grave No. 86 showed no macromorphological evidence of
178 tuberculosis (Table 1).

179 The most frequent lesions were periosteal reactions on the visceral rib surfaces and abnormal
180 vertebral vascularisation. Ten cases of superficial vertebral changes were detected (Table 1). With
181 the exception of three specimens (two mature males and one elderly female), the affected
182 individuals belong to younger age groups: one Infans II, three juveniles and three young adult
183 males. Eight individuals exhibited hypervascularisation of the anterior aspect of vertebral bodies,
184 while lytic vertebral lesions were revealed in only two cases.

185 As for rib changes, eight individuals (one juvenile, four adults, two mature and one elderly)
186 showed signs of periosteal appositions on the visceral costal surfaces (Table 1). In the majority of
187 the cases, rib periostitis showed a woven-remodelled character, indicating a less active process
188 generating these pathological changes. In two other cases (grave No. 17 and grave No. 212) it was
189 noticed that the visceral surfaces of ribs had a roughened texture.

190 Endocranial alterations were revealed in five individuals only (Table 1). Except for a mature
191 male specimen (grave No. 33), the affected individuals represent younger age groups: one juvenile
192 and three young adults (one male and two females). Concerning lesion morphology, abnormal
193 blood vessel impressions on the internal surface of the skull were observed in three of the five
194 cases, though the endocranial lamina of grave No. 22 exhibited small granular impressions similar

195 to those described by Schultz⁵ and in the skeleton of a young adult female individual (grave No.
196 233) *serpens endocrania symmetrica* (SES) was identified.

197 With the exception of two cases (grave No. 88 and grave No. 188), an association of different
198 alterations could be detected. Atypical or early-stage TB changes were accompanied by stress
199 factors in a number of cases: *cribra orbitalia* (mainly the porotic form) was observed in seven
200 cases, while long bone periostitis occurred in six cases (Table 1). Long bone periostitis appeared
201 mostly on femora and tibiae, but in three cases the long bones of the upper extremities were also
202 affected.

203 3.2 Biomolecular Analyses

204 The aDNA amplification studies gave positive results for nine of the 20 graves investigated, but
205 for only one of the four “classical TB cases” (Table 1). Full data of the aDNA analysis are provided
206 in Supplementary data. Total mycolic acid (MA) profiles are recorded in Fig. 1 that also includes a
207 summary of the overall lipid biomarker and aDNA results. All the MA profiles were too weak to
208 allow further diagnostic analyses, by sequential normal and reverse phase HPLC.^{11,29} Material from
209 five graves (Nos. 33, 66, 154, 188, 212) yielded no MAs. Fig. 2 shows three representative profiles
210 of mycolipenic (ML) and mycocerosic (MC) acids; full data are provided in Supplementary Figures
211 S3, S4 and S5.

212 The results of the lipid biomarker analyses could be placed into 6 groups (Table 1, Figs. S3-5).
213 Group 1 (grave Nos. 22, 86, 88, 134) had clear evidence of all three MA, ML and MC lipid
214 biomarker classes; grave No. 22, however, also included C₃₃ and C₃₄ mycocerosates, indicative of
215 leprosy. The major Group 2 (grave Nos. 12, 17, 48, 65, 90, 189, 215) was characterised by the
216 presence of a clear signal for mycolipenate (ML), with less convincing evidence for the other MA
217 and MC classes. Group 3 (grave Nos. 66, 188) had two representatives with good ML, weak MCs,
218 but no MA; a single member of Group 4 (grave No. 154) had only a poor ML signal. Four

219 representatives in Group 5 (grave Nos. 38, 92, 116, 233) provided weak inconclusive evidence for
220 ML and MC biomarkers. Final Group 6 (grave Nos. 33, 212) lacked any evidence of mycobacterial
221 lipid biomarkers. A close correlation with the aDNA data was not observed. Only one (grave No.
222 88) of four in the best Group 1 lipid class gave amplified DNA. Correlation was better for the
223 Group 2 lipid class with four of seven having aDNA. In the less strong or negative lipid Groups 3-6,
224 only one grave in each group had a positive aDNA result.

225 **4. Discussion and conclusions**

226 In 19 out of the 20 skeletons from Bélmegeyer-Csömöki domb a range of macromorphological
227 changes, indicative of tuberculosis, were observed. Only nine of the 20 graves yielded *M.*
228 *tuberculosis* aDNA on amplification. Lipid biomarker evidence for *M. tuberculosis* was discerned
229 in all but two of the specimens, but the strength and conclusiveness of the lipid signals could be
230 allocated to five levels (Groups 1-5) (Fig. 2). Taken by themselves, the weak total mycolic acid
231 profiles (Fig. 2) cannot be regarded as positive evidence for ancient tuberculosis. The constituents
232 of the profiles are significantly smaller than those of standard *M. tuberculosis*, suggesting either
233 considerable degradation or the presence of environmental mycobacteria. The former alternative is
234 favoured, as the two specimens (grave Nos. 33, 212) that lacked any evidence of mycolipenate
235 (ML) and mycocerosate (MC) biomarkers (Table 1), showed no evidence of any mycolates (Fig. 2).
236 Given that assumption, the MA profiles provide background support for mycobacterial infection.

237 The most positive evidence for the presence of tuberculosis resides in the MLs, which were
238 found to be usually, as strong as, or stronger than the MCs, an exception being grave No. 88 with an
239 excellent MC profile. Indeed in grave No. 154 the only lipid biomarker evidence is a very weak ML
240 signal; this is probably genuine as aDNA was amplified from this sample.

241 Of five classical tuberculosis cases (Table 1) with skeletal alterations characteristic for advanced
242 stage TB, one only (grave No. 189) was positive for MTBC DNA with clear lipid biomarker

243 support (Fig. 2; Table 1). Four of the diagnosed classical TB cases were DNA negative. However,
244 in three of these negative cases (grave Nos. 65, 90, 215) the diagnosis of skeletal tuberculosis was
245 confirmed by lipid biomarker analysis with quite strong evidence (Fig. 2). For grave No. 38, lipid
246 biomarker data were weak.

247 For cases, showing atypical or early-stage TB lesions (Table 1), many of the biomarker results
248 were inconsistent. The best lipid profiles (Group. 1) were recorded for grave Nos. 22, 86, 88 and
249 134, but only the very fragmented material from grave No. 88 was supported by aDNA.
250 Interestingly, grave No. 22 appeared to be a co-infection with tuberculosis and leprosy, the former
251 being confirmed with a strong mycolipenate peak and the latter by C₃₃ and C₃₄ mycocerosates (Fig.
252 2). The next Group 2 lipid biomarker level, with clear ML backed up by MCs in seven graves (Nos.
253 12, 17, 48, 65, 90, 189, 215) was supported by aDNA in three atypical cases (grave Nos. 12, 17, 48)
254 in addition to the classical case in grave No. 189 (Table 1). Only one (grave No. 66) of the two
255 Group 3 biomarker level specimens had aDNA support, but both graves (Nos. 66, 188) had good
256 ML backed up by weak but clear MCs. Dropping down to the single lipid biomarker Group 4
257 representative (grave No. 154), as mentioned above, aDNA amplification was supported by a weak
258 but clear ML. The four graves (Nos. 38, 92, 116, 233) assigned to lipid Group 5 had only minimal
259 ML and MC evidence but aDNA was obtained from No. 92. Although grave No. 33 was MTBC
260 DNA positive, negative lipid profiles were recorded. A juvenile male (grave No. 212.) was the only
261 specimen showing atypical or early-stage TB lesions, where the biomolecular analyses gave
262 negative results for the presence of both MTBC DNA and lipid biomarkers. The presence of
263 mycolic acid biomarkers in material from grave No. 65 was previously suggested³⁰ but the scientific
264 basis for such a diagnosis has been dismissed.³¹

265 Morphological assessment, detection of ancient DNA and demonstration of *M. tuberculosis*
266 complex cell wall lipid markers proves there was widespread TB infection in this 8th century
267 population. A variety of lesions at different stages of development were observed. The biomolecular

268 studies confirmed the presence of tuberculosis and lipid analysis also indicated a TB/leprosy
269 coinfection. Our study highlights the difficulties of demonstrating TB in these individuals from over
270 1300 years ago and the importance of using different methods is very clear. The relative success of
271 lipid biomarkers compared with aDNA is probably due to their greater stability over time. This
272 underlines the complementarity of morphological, aDNA and lipid biomarkers analyses in the
273 diagnosis of ancient TB infections.

274 **Ethical approval**

275 Not required

276 **Funding**

277 The Leverhulme Trust Project Grant F/00 094/BL (OY-CL, DEM, GSB). GSB was supported by
278 a Personal Research Chair from Mr. James Bardrick and the UK Medical Research Council. The
279 UK Engineering and Physical Sciences Research Council (EPSRC) funded the UK National Mass
280 Spectrometry Facility at Swansea University (GL, CMW). The UK National Environmental
281 Research Council (NERC) provided funding for the mass spectrometry facilities at Bristol (Contract
282 no. R8/H12/15; www.lsmsf.co.uk) (IDB). The Hungarian Scientific Research Fund OTKA (OTKA
283 Grant No. K78555 and NN 78696) provided funding for the macromorphological studies.

284 **Author contributions**

285 EM and GP conceived the study and with OS performed the macromorphological analysis. HD
286 performed the aDNA studies. DM and GB conceived the lipid work, which was performed by OL,
287 HW, IB, GL and CW. The lipid data were analyzed by DM, GB, OL and HW. EM, DM and HD
288 wrote the manuscript and all authors approved the final version.

289 **Competing interests**

290 None declared.

291

292 **References**

- 293 1. Pálfi Gy, Bereczki Zs, Ortner DJ, Dutour O. Juvenile cases of skeletal tuberculosis from the
294 Terry Anatomical Collection (Smithsonian Institution, Washington, D.C., USA). *Acta*
295 *Biologica Szegediensis* 2012; **56**:1-12.
- 296 2. Ortner DJ. *Identification of paleopathological conditions in human skeletal remains*. San
297 Diego: Academic Press, 2003.
- 298 3. Dutour O. Archaeology of human pathogens: palaeopathological appraisal of
299 palaeoepidemiology. In: Raoult D, Drancourt M, editors. *Paleomicrobiology: past human*
300 *infections*. Berlin, Heidelberg: Springer-Verlag GmbH, 2008. p. 125-144.
- 301 4. Baker BJ. Early manifestations of tuberculosis in the skeleton. In: Pálfi Gy, Dutour O, Deák J,
302 Hutás I, editors. *Tuberculosis: past and present*. Szeged & Budapest: TB Foundation & Golden
303 Book Publisher, 1999. p. 301-307.
- 304 5. Schultz M. Paleohistopathology of bone: a new approach to the study of ancient diseases.
305 *Yearbook of Physical Anthropology* 2001; 44:106-147.
- 306 6. Hershkovitz I, Greenwald CM, Latimer B, Jellema LM, Wish-Baratz S, Eshed V, Dutour O,
307 Rothschild BM. Serpens Endocrania Symmetrica (SES): a new term and a possible clue for
308 identifying intrathoracic disease in skeletal populations. *American Journal of Physical*
309 *Anthropology* 2002; 118:201-216.
- 310 7. Pálfi Gy. Paleoepidemiological reconstruction of tuberculosis with particular attention to
311 Europe. In: Bennike P, Bodzsár E, Susanne C, eds. *Biennial Books of EAA* 2002;**2**:193-210.
- 312 8. Stuart-Macadam PL. Nutritional deficiency diseases: a survey of scurvy, rickets and iron
313 deficiency anemia. In: Isçan MY, Kennedy KAR, editors. *Reconstruction of life from the*
314 *skeleton*. New York: Alan R. Liss Publisher, 1989. p. 201-222.
- 315 9. Haas CJ, Zink A, Molnár E, Szeimies U, Reischl U, Marcsik A, Ardagna Y, Dutour O, Pálfi
316 Gy, Nerlich AG. Molecular evidence for different stages of tuberculosis in ancient bone
317 samples from Hungary. *American Journal of Physical Anthropology* 2000; 113: 293-304.

- 318 10. Zink AR, Molnár E, Motamedi N, Pálfi Gy, Marcsik A, Nerlich AG. Molecular history of
319 tuberculosis from ancient mummies and skeletons. *International Journal of Osteoarchaeology*
320 2007; 17:380-391.
- 321 11. Hershkovitz I, Donoghue HD, Minnikin DE, Besra GS, Lee OY-C, Gernaey AM, Galili E,
322 Eshed V, Greenblatt CL, Lemma E, Bar-Gal GK, Spigelman M. Detection and molecular
323 characterization of 9000-year-old *Mycobacterium tuberculosis* from a Neolithic settlement in
324 the Eastern Mediterranean. *PLoS ONE* 2008; 3:e3426.
- 325 12. Pósa A, Maixner F, Lovász G, Molnár E, Bereczki Zs, Perrin P, Zink AR, Pálfi Gy. Revision of
326 tuberculous lesions in the Bácsalmás-Óalmás series – preliminary morphological and
327 biomolecular studies. *Anthropologischer Anzeiger* 2012, doi: 10.1127/0003-5548/2012/0260.
- 328 13. Pálfi Gy, Csernus Z. Arthrite infectieuse ankylosante dans une série du VIII^e siècle en Hongrie.
329 *Paléobios* 1990; 6:37-41.
- 330 14. Pálfi Gy. The osteoarchaeological evidence of vertebral tuberculosis in the 8th century. *Acta*
331 *Biologica Szegediensis* 1991; 37:101-105.
- 332 15. Pálfi Gy, Marcsik A, Kovács J. Lumbosacral and hip tuberculosis in a Migration period
333 skeleton. *Journal of Paleopathology* 1992; 4:179-184.
- 334 16. Marcsik A, Molnár E, Ósz B. *Specifikus fertőző megbetegedések csontelváltozásai történeti*
335 *népesség körében*. Szeged: JatePress, 2007.
- 336 17. Medgyesi P. Késő avar temető Béli-megyér-Csömöki dombon (Előzetes jelentés).
337 Spätawarenzeitliches Gräberfeld auf Hügel Béli-megyér-Csömök (Vorbericht). In: *A Móra*
338 *Ferenc Múzeum Évkönyve*. Szeged: 1991. p. 241-256.
- 339 18. Medgyesi P. Béli-megyér. In: Jankovich BD, editor. *Magyarország régészeti topográfiája. 10.*
340 *Békés megye régészeti topográfiája*. Budapest: Akadémiai Kiadó, 1998. p. 342-348.
- 341 19. Taylor GM, Mays SA, Huggett JF. Ancient DNA (aDNA) studies of man and microbes:
342 general similarities, specific differences. *International Journal of Osteoarchaeology* 2010;
343 20:747-751.

- 344 20. Donoghue HD, Marcsik A, Matheson C, Vernon K, Nuorala E, Molto J, Greenblatt C,
345 Spigelman M. Co-infection of *Mycobacterium tuberculosis* and *Mycobacterium leprae* in
346 human archaeological samples—a possible explanation for the historical decline of leprosy.
347 *Proceedings of the Royal Society B: Biological Sciences* 2005; 272:389-394.
- 348 21. Poinar HN, Hofreiter M, Spaulding WG, Martin PS, Stankiewicz BA, Bland H, Evershed EP,
349 Possnert G, Pääbo S. Molecular coproscopy: dung and diet of the extinct ground sloth
350 *Nothrotheriops shastensis*. *Science* 1998; 281:402-406.
- 351 22. Eisenach KD, Cave MD, Bates JH, Crawford JT. Polymerase chain reaction amplification of a
352 repetitive DNA sequence specific for *Mycobacterium tuberculosis*. *The Journal of Infectious*
353 *Diseases* 1990; 161:977-981.
- 354 23. Taylor GM, Stewart GR, Cooke M, Chaplin S, Ladva S, Kirkup J, Palmer S, Young DB.
355 Koch's Bacillus—a look at the first isolate of *Mycobacterium tuberculosis* from a modern
356 perspective. *Microbiology* 2003; 149:3213-3220.
- 357 24. Évinger S, Bernert Zs, Fóthi E, Wolff K, Kővári I, Marcsik A, Donoghue HD, O'Grady J, Kiss
358 KK, Hajdu T. New skeletal tuberculosis cases in past populations from Western Hungary
359 (Transdanubia). *HOMO – Journal of Comparative Human Biology* 2011; 62:165-183.
- 360 25. Abu Al-Soud W, Rådström P. Effects of amplification facilitators on diagnostic PCR in the
361 presence of blood, feces and meat. *Journal of Clinical Microbiology* 2000; 38:4463-4470.
- 362 26. Hajdu T, Donoghue HD, Bernert Zs, Fóthi E, Kővári I, Marcsik A. A case of spinal
363 tuberculosis from the Middle Ages in Transylvania (Romania). *Spine* 2012; 37:e1598-1601.
- 364 27. Taylor GM, Worth DR, Palmer S, Jahans K, Hewinson RG. Rapid detection of *Mycobacterium*
365 *bovis* DNA in cattle lymph nodes with visible lesions using PCR. *BMC Veterinary Research*
366 2007; 3:12-22.
- 367 28. Donoghue HD, Spigelman M, O'Grady J, Szikossy I, Pap I, Lee OY-C, Wu HHT, Besra GS,
368 Minnikin DE. Ancient DNA analysis – an established technique in charting the evolution of
369 tuberculosis and leprosy. In: *Proceedings of ICEPT-2 – The Past & Present of Tuberculosis: a*

370 *multidisciplinary overview on the origin and evolution of TB. One of the Conference series on*
371 *the occasion of the 75th Anniversary of Albert Szent-Györgyi 's Nobel Prize Award, Szeged,*
372 *Hungary, 22nd – 25th March 2012.*

373 29. Lee OY-C, Wu HHT, Donoghue HD, Spigelman M, Greenblatt CL, Bull ID, Rothschild BM,
374 Martin LD, Minnikin DE, Besra GS. *Mycobacterium tuberculosis* complex lipid virulence
375 factors preserved in the 17,000-year-old skeleton of an extinct bison, *Bison antiquus*. *PLoS*
376 *ONE* 2012; 7:e41923.

377 30. Mark L, Patonai Z, Vaczy A, Lorand T, Marcsik A. High-throughput mass spectrometric
378 analysis of 1400-year-old mycolic acids as biomarkers for ancient tuberculosis infection. *J*
379 *Archaeol Sci*, 201037, 302–305.

380 31. Minnikin D, Lee OY-C, Wu HHT, Besra G, Donoghue H. Molecular biomarkers for ancient
381 tuberculosis. In: Cardona, P-J. (ed.) *Understanding tuberculosis - deciphering the secret life of*
382 *the bacilli*. Rijeka, Croatia: InTech Open Access Publisher 2012. p. 3–36. ISBN-13: 978-953-
383 307-946. Available from: [http://www.intechopen.com/articles/show/title/molecular-](http://www.intechopen.com/articles/show/title/molecular-biomarkers-for-ancient-tuberculosis)
384 [biomarkers-for-ancient-tuberculosis](http://www.intechopen.com/articles/show/title/molecular-biomarkers-for-ancient-tuberculosis)

385

386 **Figure legends**

387 Figure 1. Reverse phase fluorescence HPLC of total mycolates. The grave numbers are
388 accompanied (in brackets) by the amount of sample analysed (mg). The “Lipid” column indicates
389 the diagnostic power of mycolate (MA), mycolipenate (ML) and mycocerosate (MC) lipid
390 biomarkers: ++++ (group 1), clear evidence of MA, ML and MC; +++ (group 2), clear ML signal
391 with less strong MA and MC; ++ (group 3), good ML, weak MC and no MA; + (group 4), only a
392 clear weak ML peak; +? (group 5), weak inconclusive ML and MC with some MA support; -
393 (group 6), no evidence of mycobacterial lipids; ++++*, strong *M. tuberculosis* lipid signals with
394 additional MC indicating *M. leprae*. The “aDNA” list records the presence of amplified DNA
395 fragments.

396 Figure 2. Representative selected ion monitoring (SIM) negative ion-chemical ionization gas
397 chromatography-mass spectrometry (NI-CI GC-MS) profiles of mycolipenate and mycocerosates.
398 **A, C, E** grave Nos. 88 (Bristol University), 134 and 22 (Swansea University); **B, C** *M. tuberculosis*
399 standard recorded at Bristol and Swansea, respectively; **F**, *M. leprae* standard recorded at Swansea.
400 Ions monitored are exemplified by $C_{27} m/z 407$ and $C_{27} m/z 409$, representing C_{27} mycolipenate and
401 C_{27} mycocerosate, respectively. Relative intensities (**bold in brackets**) are shown normalized to the
402 major component (**100**).

403

404 **Table 1.** Data for material investigated from Bélmegyer-Csömöki domb.

CLASSICAL TB CASES											
Gr No	sex	age at death	macromorphology			aDNA	lipid biomarkers				
			ST	CT	GT		MA	ML	MC		
38	F	16□18	□	+	□	□	+	+?	+?		
65	F	Maturus	+	□	□	□	+?	+	+		
90	M	57□62	+	+	□	□	+	+	+?		
189	M	25□28	+	□	□	+	+	+	+?		
215	F	55□60	□	□	+	□	+?	+	+		
ATYPICAL (EARLY-STAGE) TB CASES											
Gr No	sex	age at death	macromorphology					aDNA	lipid biomarkers		
			SVC	RP	EL	LBP	CO		MA	ML	MC
12	M	33□39	□	+++	□	+	□	+	+?	++	+?
17	M	22□25	+	+	+	+	+	+	+?	++	+?
22	undet.	16□18	+	□	+	□	□	□	+	++	+
33	M	40□45	+	□	+	+	+	+	□	□	□
48	M	55□60	+	+	□	+(DP)	□	+	+	+	+
66	F	61□67	+	+	□	□	□	+	□	+	+?
86	M	59□64	□	□	□	□	□	□	+	++	+
88	F	40□45	□	+++	□	□	□	+	+	+	+++
92	M	20□25	+	+++	□	+	□	+	+	+?	+?
116	F	25□30	□	+++	+	+++ (DP)	□	□	+	+?	+?
134	F	16□18	+	□	□	□	+	□	++	+	+
154	M	20□24	+	□	□	□	+	+	□	+?	□

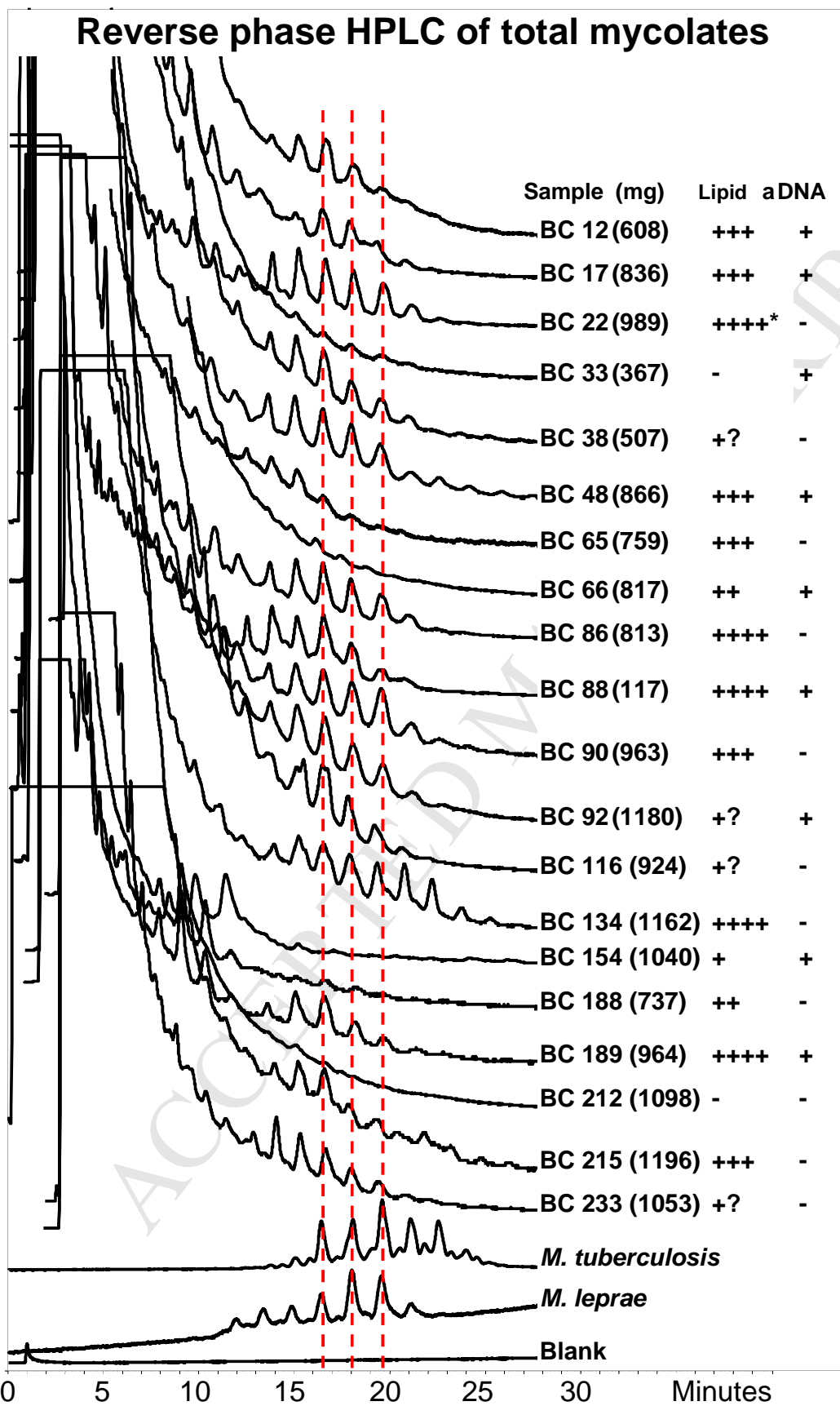
188	undet.	7	+	□	□	□	□	□	□	++	+	
212	M	18□20	+	+	□	□	□	□	□	□	□	
233	F	23□25	□	□	+	□	□	□	□	+	+?	+?

405

406 **Gr No** = grave No; **F** = female; **M** = male; **undet.** = undeterminable sex; **ST** = spondylitis
407 tuberculosa; **CT** = coxitis tuberculosa; **GT** = gonitis tuberculosa; **SVC** = superficial vertebral
408 changes; **RP** = rib periostitis; **EL** = endocranial lesions; **LBP** = long bone periostitis; **CO** = cribra
409 orbitalia; **DP** = diffuse periostitis; **MA** = mycolates; **ML** = mycolipenate; **MC** = mycocerosates.

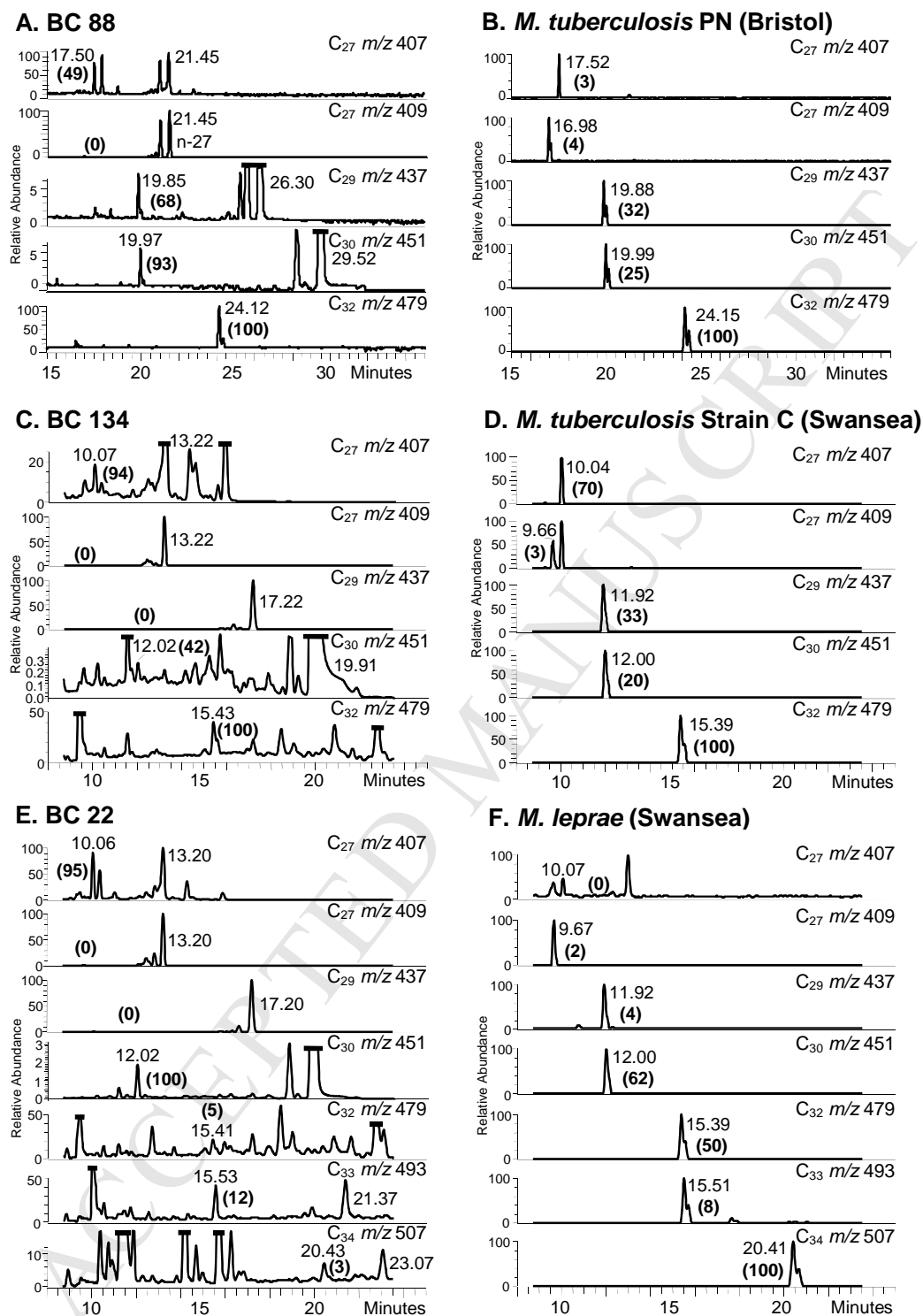
410

411 Figure 1



412

21

413 **Figure 2**

414

SUPPLEMENTARY DATA

Paleopathological analysis

The distinction between classical and atypical or early-stage TB cases is shown in the figures below.

Legend to Figure S1**Classical TB cases**

- a) Tuberculous spondylitis healed with gibbus formation (L1-L3) - Grave No. 65. (female, mature)
- b) Severe destruction of the 3rd vertebral body (inferior view) - Grave No. 65. (female, mature)
- c) Lumbosacral tuberculosis: severe erosion of the ventral sacral surface (traces of cold abscess) - Grave No. 90. (male, elderly)
- d) *Coxitis tuberculosa*: complete destruction and remodelling of the acetabulum - Grave No. 90. (male, elderly)

a)



b)



c)



d)



Legend to Figure S2**Atypical or early-stage TB changes**

- a) Periosteal apposition on the visceral costal surface – Grave No. 88. (female, mature)
- b) Maze like surface excavation (*serpens endocrania symmetrica*)- Grave No. 233. (female, young adult)
- c) Abnormal vertebral vascularisation - Grave No. 92. (male, young adult)

ACCEPTED MANUSCRIPT

a)



b)



c)



Details of DNA extraction

(a) Disaggregation of samples and DNA extraction

A small quantity (22–78mg) of each sample was crushed by a sterile pestle in a mortar and added to 400µl of Proteinase K/EDTA. Samples were processed in batches of 7 plus a negative extraction control. The slurry was incubated at 56°C²⁴, and mixed on a bead beater daily. When the sample was solubilised, it was divided and one aliquot treated with 40µl of 0.1mol⁻¹ of N-phenacylthiozolium bromide (PTB), to cleave any covalent cross-links thus enabling DNA strand separation and amplification²¹. Sample tube contents were transferred into separate 9ml tubes of NucliSens® (bioMérieux) lysis buffer containing 5mol⁻¹ guanidium thiocyanate and incubated for 1–3 days at 56°C. To complete the disruption of bone and any mycobacterial cell wall remnants, samples were boiled, then snap-frozen in liquid nitrogen and thawed in a 65°C waterbath. This procedure was repeated twice. Sample tubes were centrifuged at 5000g for 15 min at 5°C and the supernatants carefully removed into clean, sterile tubes. DNA was captured by adding 40µl silica suspension (NucliSens®) and mixing on a rotator wheel for 1 h. Tube contents were centrifuged and silica pellets washed once with wash buffer (NucliSens®), twice with 70% (v/v) ethanol (□20°C) and once with acetone (□20°C). After drying in a heated block, DNA was eluted using 60µl elution buffer (NucliSens®), aliquoted and used immediately or stored at □20°C. Silica supernates (500µl) from PTB-negative samples were also collected from the 9ml tubes of lysis buffer, and the 2.0ml screw-capped Eppendorf tubes used to wash the silica. After chilling at 5°C, supernates were mixed vigorously for 20 s with 200µl of Protein Precipitation Solution (SLS Ltd., UK) and centrifuged for 3min at 10,000g. Any pellet was discarded and 600µl isopropanol (□20°C) added to 550µl of each supernate. Tubes were mixed by inversion 50 times and spun 3min. Supernates were discarded and tubes washed once with 500µl 70% ethanol (□20°C). After draining, tubes were dried in a heating block. Any precipitated DNA was re-hydrated with 60µl elution buffer (NucliSens®), aliquoted and used immediately or stored at □20°C. Negative extraction controls were processed in parallel with the test samples.

(b) DNA amplification and detection

Two specific regions of the MTBC were targeted in the repetitive elements IS6110 (1–25 copies/cell) and IS1081 (6 copies/cell). The IS6110 primers had a target region of 123 bp²² and the IS1081 primers designed by Taylor *et al.*²³ produce an amplicon of 113 bp. Later,

specific *M. tuberculosis* primers and a fluorescent probe were used²⁴ to enable shorter DNA fragments to be detected in a real-time PCR reaction.

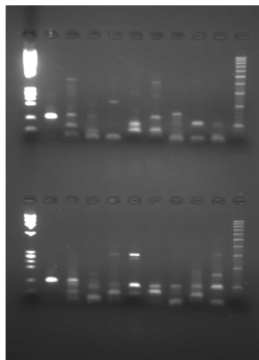
(c) The PCR conditions

The PCR mix included 2mM bovine serum albumin (BSA) to reduce PCR inhibition²⁵ and 2.0mM MgCl₂. PCR assays were initially run at an annealing temperature of 58°C and amplified DNA was examined by agarose gel electrophoresis.²⁶ Subsequently, amplification was performed in a final volume of 25µl using a RotorGene© 3000 (Qiagen) real-time platform²⁷, to enable the detection of DNA using SYBR Green and melt analysis or specific primers with fluorescent probe. Annealing was at 60°C. A hot-start Taq polymerase was used to minimize non-specific primer and template binding. Negative DNA extraction and PCR controls were processed alongside the test samples.

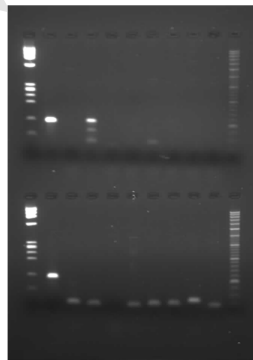
(d) Results

Single-stage PCRs with outer primer pairs

Gel with IS6110 PCR products



Gel with IS1081 PCR products



Key to abbreviations:

EC = negative extraction control; s = silica supernate (fluid left in 2 ml tubes after silica spun down, normally short aDNA fragments); LVs = large volume silica supernate (fluid left in 9 ml lysis buffer tubes after silica spun down, short aDNA fragments); wb = water blank negative control in PCR.

Lanes (left to right): 1: Phi X-174 *Hae*III markers; 11: 20bp and 100bp molecular markers

Top row: 2: +ve control; 3: BC-12s; 4: BC-12 LVs; 5: wb1; 6: BC-17s; 7: BC-17 LVs; 8: BC-22s; 9: wb2; 10: BC-22 LVs;

Bottom row: 2: +ve control; 3: BC-33s; 4: BC-33 LVs; 5: BC-38s; 6: ECs; 7: BC-38 LVs; 8: BC-48s; 9: BC-48 LVs; 10: EC LVs;

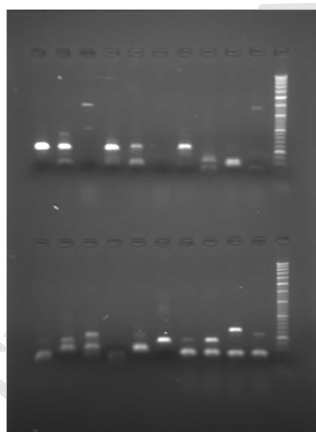
Conclusions:

IS6110: possible weak positives with BC-12 LVs and BC-17 LVs. Positive with BC-33s.

Non-specific bands from BC-12s, BC-22s, BC-33 LVs, and BC-48 LVs. Others negative.

IS1081: positive with BC-12 LVs. All other samples (except positive controls) were negative

Single-stage *IS1081* PCRs using inner primers (113 bp)



Lanes (left to right): 11: 20bp and 100bp molecular markers

Top row: Lane 1: +ve control; 2: BC-12; 3: wb5; 4: BC-12+; 5: BC-17; 6: wb6; 7: BC-17+; 8: BC-22; 9: BC22+; 10: wb7.

Bottom row: Lane 1: BC-33; 2: BC-33+; 3: BC-48; 4: wb8; 5: BC-48+; 6: EC; (lanes 7–10: different samples and another PCR)

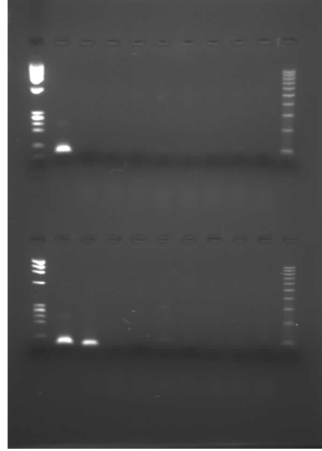
Conclusions:

Positives from samples BC-12, BC-12+, BC-17, BC-17+, BC-48.

Doubtful results from BC-22, BC-22+ (very faint trace) and BC-48+.

Negatives from BC-33 and 33+, and all water blanks.

BC-51 was examined separately for MTB *IS1081* but was negative.

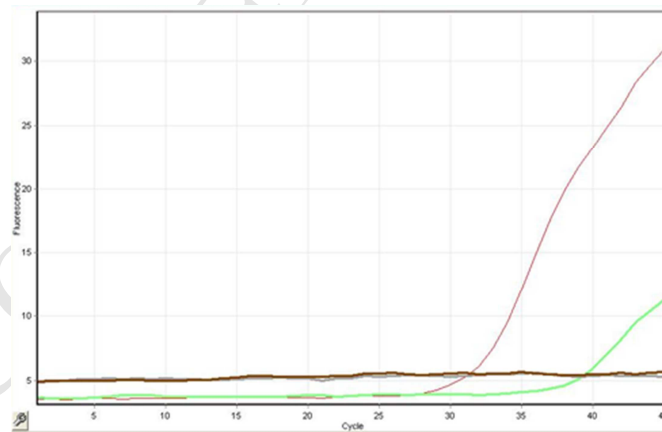
Nested IS6110 PCRs using inner primer pair

Samples loaded in the same order as above, using the stage 1 PCR products that were re-amplified for a further 25 cycles.

Conclusions:

Positive and negative controls were satisfactory. Only BC-33s was positive.

Real-time experiments were also carried out with the same primers and melt analysis. Results are summarized at the end of the document.

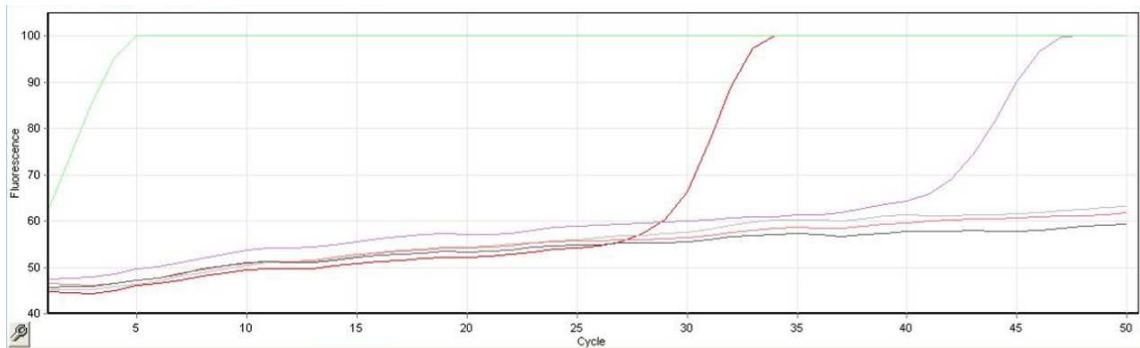
Real-time PCR with IS1081 primers and probe

The lower the cycle threshold (C_t) the greater the quantity of target aDNA in the sample. In this image, the positive samples in order of their C_t was as follows:

Positive control (a 1/10 dilution of extract from a Vác mummy) C_t 32 cycles

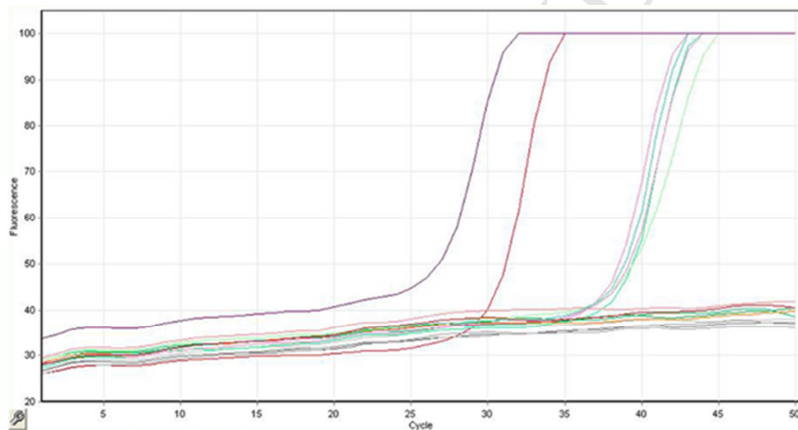
BC-189+ (+ indicates the DNA was extracted using PTB) C_t 39 cycles

Negatives were obtained from BC-12, BC-22, BC-116+, BC-116, BC-134+, BC-134, BC-134s, BC-188+, BC-188, BC-189, BC-215, wb1, wb2, wb3, wb4, EC, EC1, EC+, ECs



In this experiment a nested PCR was performed on the PCR product from BC-189+ which explains the high level of signal at the start of the reaction. The positive control had a C_t of 28 and sample BC-92 had a C_t of 41.

Negatives were obtained from BC-22, BC-65+, BC-65, BC-66+, BC-66, BC86+, BC-86, BC-88+, BC-88, BC-90+, BC-90, BC-92+, BC-154+, BC-154, wb1, wb2, wb3, wb4, EC+, EC.



The positive control had a C_t of 28.6, BC-66s: 36.6, BC-86s: 36.9, BC-92: 36.0, BC-92s: 36.3, and BC-154: 36.1. Individual screenshots are available for each positive sample. Negative results were obtained from BC-65s, BC-86s, BC-90s, wb, EC and ECs. These results were confirmed by agarose gel electrophoresis.

Overall findings for *M. tuberculosis* complex in these samples

Positives with one or both target regions:

BC-12, BC-17, BC-33, BC-48, BC-66, BC-88, BC-92, BC-154, BC-189

Negative (but cannot exclude poor preservation):

BC-22, BC-38, BC-65, BC-86, BC-90, BC-116, BC-134, BC-188, BC-212, BC-215, BC-233

Analysis of mycolipenate and mycocerosates

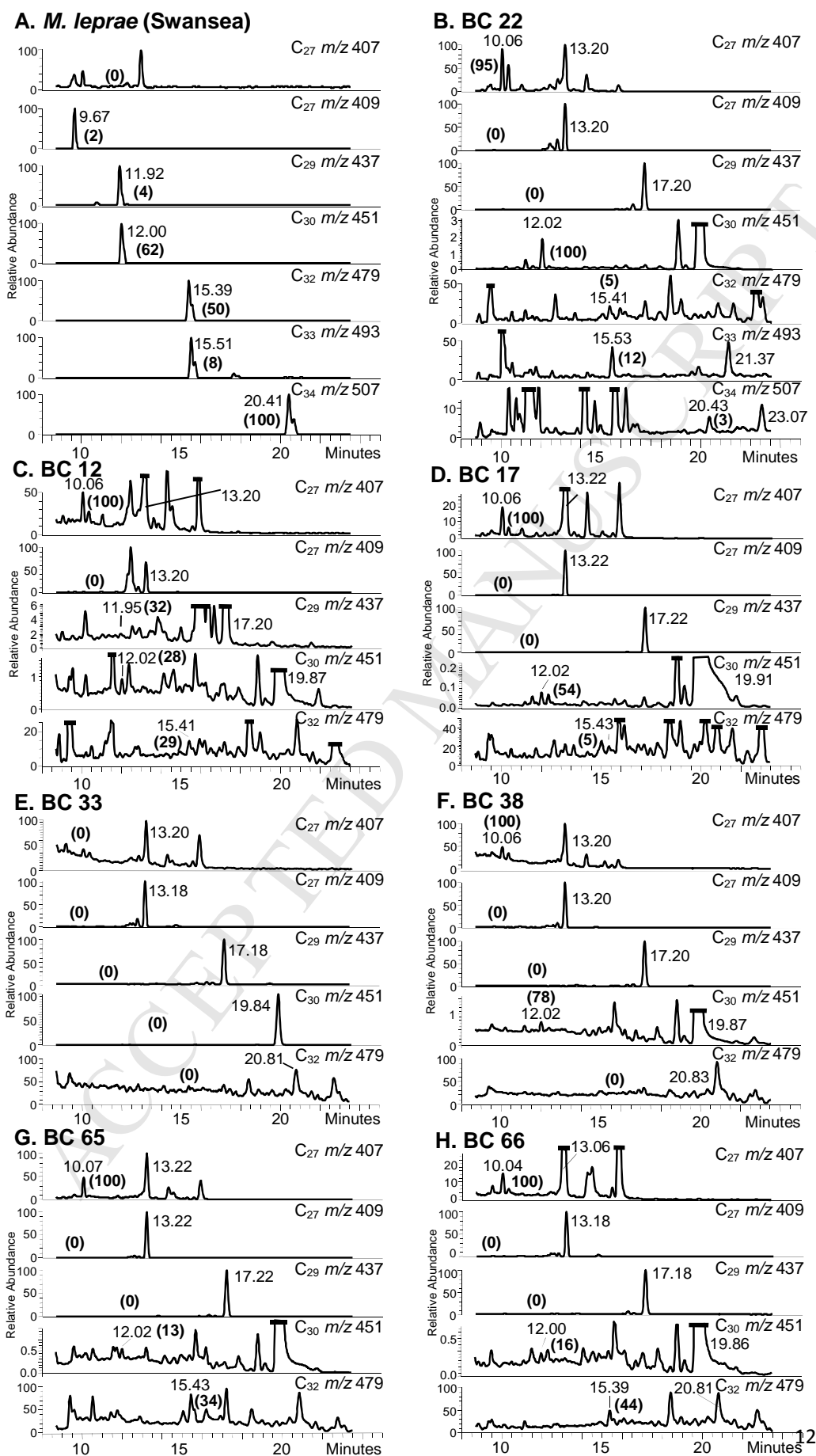
The initial analyses were performed at Bristol University, using a ThermoFinnigan MAT95 XP-Trap mass spectrometer, fitted with a Phenomenex Zebron ZB-5 (5% phenyl, 95% dimethylpolysiloxane) capillary column (30 m × 0.25 mm i.d. × 0.25 µm film thickness) using He as carrier gas (constant flow mode 1 ml min⁻¹) and ammonia as the CI reagent gas. A GC oven temperature gradient from 200 to 300°C at 6.7°C min⁻¹ was used, the final temperature being held for 20 min. The ion source temperature was 250°C, the injector 300°C and the transfer line 300°C. Selected ion monitoring (SIM) was used for mycocerosate ions at m/z 367.6311 (C₂₄), 395.6844 (C₂₆), 409.7111 (C₂₇), 437.7645 (C₂₉), 451.7911 (C₃₀), 479.8445 (C₃₂), 493.8712 (C₃₃) and 507.8978 (C₃₄); additionally, m/z 407.6952 was monitored for the presence of C₂₇ mycolipenic acid. Later studies were carried out at Swansea University with the same Phenomenex Zebron ZB-5 column, using He as carrier gas. PFB esters, on NICI-GCMS, fragment to produce negative carboxylate [M – H]⁻ ions, which can be detected at high sensitivity. Selected ion monitoring (SIM) was used to search for mycocerosate carboxylate ions at m/z 367.6311 (C₂₄), 395.6844 (C₂₆), 409.7111 (C₂₇), 437.7645 (C₂₉), 451.7911 (C₃₀), 479.8445 (C₃₂), 493.8712 (C₃₃) and 507.8978 (C₃₄).²⁹ Additionally, m/z 407.6952 was monitored for the presence of the C₂₇ mycolipenate carboxylate ion.²⁹ Partial racemisation of mycocerosates during the alkaline hydrolysis leads to the formation of diastereoisomers, which resolve on gas chromatography to give characteristic doublets; in contrast, mycolipenates are singlets as they cannot racemise.²⁹

Legend to Figure S3

Selected ion monitoring (SIM) negative ion chemical ionisation (NI-CI) gas chromatography mass spectrometry (GC-MS) of pentafluorobenzyl esters (Swansea University). **A.** Standard *M. leprae* (Swansea University); **B-H.** Samples extracted from graves (BC) 22, 12, 17, 33, 38, 65, 66, respectively. Intensities (**bold in brackets**) are normalised to the major component (**100**).

ACCEPTED MANUSCRIPT

Figure S3

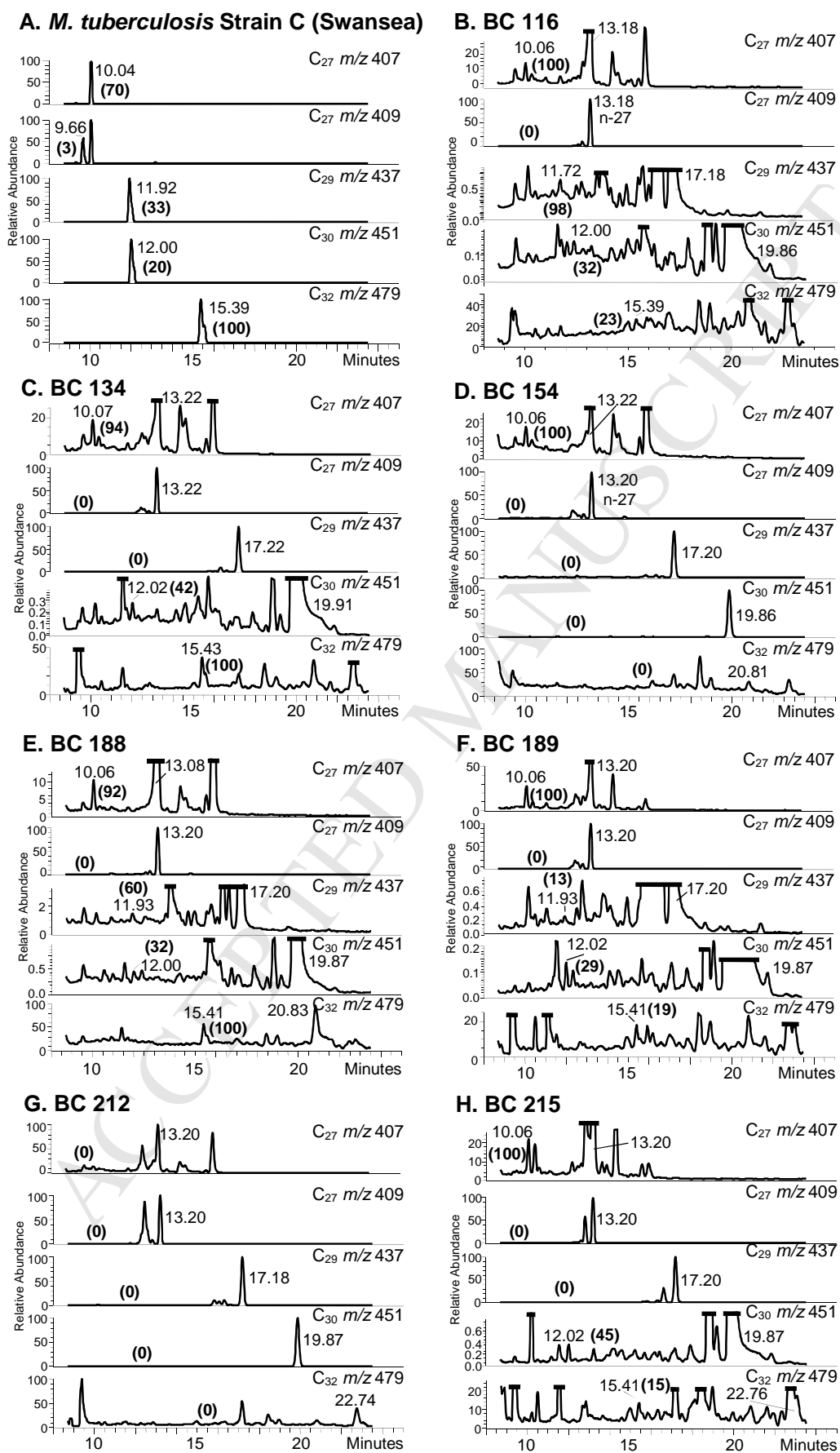


Legend to Figure S4

Selected ion monitoring (SIM) negative ion chemical ionisation (NI-CI) gas chromatography mass spectrometry (GC-MS) of pentafluorobenzyl esters (Swansea University). **A.** Standard *M. tuberculosis* (Strain C) (Swansea University); **B-H.** Samples extracted from graves (BC) 116, 134, 154, 188, 189, 212, 215, respectively. Intensities (**bold in brackets**) are normalised to the major component (**100**).

ACCEPTED MANUSCRIPT

Figure S4



Legend to Figure S5

Selected ion monitoring (SIM) negative ion chemical ionisation (NI-CI) gas chromatography mass spectrometry (GC-MS) of pentafluorobenzyl esters (Bristol University). **A-F**. Samples extracted from graves (BC) 48, 86, 88, 90, 92, 233, respectively. Intensities (**bold in brackets**) are normalised to the major component (**100**).

ACCEPTED MANUSCRIPT

Figure S5

